*Physics – Uspekhi* **48** (8) 781 – 796 (2005) 

*REVIEWS OF TOPICAL PROBLEMS*

PACS numbers: **76.60. – k**, **82.56. – b**, 82.56.Pp

# Exchange NMR spectroscopy in solids: application in large-scale conformational biopolymer dynamics studies

A G Krushelnitsky

DOI: 10.1070/PU2005v048n08ABEH002199

## Contents



**Abstract. The exchange NMR experiment compares resonant frequencies of a magnetic nucleus before and after the so-called mixing time, thereby gaining molecular dynamics information on millisecond and second correlation time scales. Although exchange NMR experiments on solutions have a long history, conducting them on solids presents methodological challenges, and it was only in the late 1990s that solid-state exchange spectroscopy matured to the level where such complex entities as biopolymers could be addressed. In this review, major methodological advances in the field are examined and the application of exchange NMR experiments to conformational molecular dynamics of solid-state biopolymers is described.**

## 1. Introduction

During the few last decades, proteins have become a popular, if not the most popular, biological object investigated by a variety of physical methods. One of the principal aims of this work is to promote better understanding of the molecular mechanisms underlying the biological functioning of proteins. Protein studies have numerous practical implications besides their purely theoretical interest. Knowledge of the ways a protein performs its function (enzymatic, inhibitory, transport, mechanico-chemical, etc.) allows us to modify the protein or impart a new property to a protein molecule of importance for biotechnology and medicine.

Investigations into the mechanisms of protein functioning can be categorized, even if arbitrarily, into two mutually related groups. One includes structural studies, while the other conformational protein dynamics studies. There is little doubt today that both lines of research are crucial for understanding the molecular basis of the biological functions of proteins. Historically, structural studies started much earlier than dynamical ones, which accounts for the greater degree of progress in this field compared with molecular dynamics studies. The initial impetus for the development of structural studies came from the pioneering decoding of the spatial structure of hemoglobin, a globular protein, using X-ray diffraction analysis [1]. In 1962, Max Perutz was awarded the Nobel Prize in Chemistry for this work. Since then, thousands of structures of various proteins have been decoded by the same method. The new burst of interest in protein structural studies dates from the late 1980s and 1990s, aroused by the advent of another powerful method for investigating protein structures, namely, high-resolution multidimensional and multinuclear NMR spectroscopy of biological macromolecules in solutions [2]. The 2002 Nobel Prize in Chemistry was awarded for this work to the Swiss researcher Kurt Wüthrich.

Although knowledge of the spatial structure of polypeptide chains opens up the possibility of understanding a great many properties of proteins, it was clear from the very beginning that it is insufficient to comprehensively explain mechanisms of protein functioning at the molecular level. It is easy to see in the example of the aforementioned hemoglobin. Its biological function consists in maintaining oxygen transport in the blood. An oxygen molecule is bound to hem, the active protein center, and is transferred in the resulting complex to target tissues. However, detailed structural analysis indicates that the binding cleft between the hem and the protein surface is too narrow for the oxygen molecule to 'squeeze through' toward the active site. Hence the hypothesis of mobile protein structure, according to which the binding cleft widens, making hem sterically accessible and permitting the protein binding to the oxygen molecule. The role of molecular dynamics in the biological functioning of hemoglobin was considered at length in a series of works published by Martin Karplus (see review [3] and references cited therein).

This is one of the simplest and most straightforward, yet far from most exhaustive, example of the importance of molecular dynamics for the realization of a biological function. Besides the regulation of the access of a ligand to a

**A G Krushelnitsky** Kazan' Institute of Biochemistry and Biophysics, Russian Academy of Sciences,
ul. Lobachevskogo 2/31, 420111 Kazan', Russian Federation
Tel. (7-8432) 31 90 37
Fax (7-8432) 92 73 47
E-mail: krushelnitsky@mail.knc.ru

Received 8 December 2004
*Uspekhi Fizicheskikh Nauk* **175** (8) 815 – 832 (2005)
Translated by Yu V Morozov; edited by A Radzig

protein, conformational mobility may be essential for molecular recognition, e.g., in barstar [4, 5] or the tryptophane-repressor [6], as well as in other biological processes. Molecular mechanisms of the involvement of molecular dynamics in biological function have been reviewed in a number of recent publications [7 – 11]. It is worth noting, however, that mechanisms underlying participation of molecular mobility in protein functioning are very intricate and sometimes difficult to explain. Thus far, there is no single approach or algorithm to facilitate the understanding of the relationship between molecular dynamic parameters and a given biological function. Indeed, such an approach may not exist in principle: the problem is very specific and requires special analysis in each concrete case.

The frequency range of atomic vibrations in proteins is rather wide. The characteristic time of the fastest movements is measured in femtoseconds and fractions of a femtosecond, and that of the slowest ones in seconds. The femtosecond range corresponds to vibrations of valence bonds and bond angles. These dynamics are largely studied by optical spectroscopy. Vibrations in the picosecond and all slower ranges are due to the conformational degrees of freedom of the protein structure — that is, dihedral (torsion) angles $\phi$ and $\varphi$ that impart flexibility to the protein backbone chain, and also dihedral angles $\chi$ responsible for the conformation of the side chains of amino acid residues. Vibrations of these angles may be very rapid, when they are associated with the motions of individual chemical groups. For example, the characteristic time of rotation of three methyl protons about the axis of symmetry of the methyl group at room temperature is measured in picoseconds, and uncorrelated low-amplitude vibrations of individual side chains, as well as small sections of the backbone chain, in nanoseconds and fractions of a nanosecond. Large-scale conformation transitions are always highly correlated changes of many degrees of freedom of proteins because they comprise rather densely packed structures having practically no free volume inside the globule. Noticeable displacements of one domain of the protein structure are always correlated with that of neighboring domains. The characteristic time of the internal dynamics of this type lies in the micro- or millisecond range. It is noteworthy that the time scale of slow dynamics coincides with the time scale of many molecular biological processes, such as binding to a substrate, catalysis, folding, etc. It is therefore natural to assume that just slow conformational dynamics play a leading role in the biological functioning of proteins and is of special interest in the biological context.

The battery of methods used up to now in the studies of protein molecular dynamics includes nuclear magnetic resonance (NMR), electron paramagnetic resonance (EPR), dielectric, fluorescent, infrared, and Mössbauer spectroscopies, neutron scattering, numerical simulation, and even X-ray diffraction analysis that yields information about the so-called B-factors, i.e., the degree of 'smearing out' of the atomic coordinates in space due to molecular mobility. However, it is generally accepted now that NMR is the most powerful and informative tool, providing a very wide range of possibilities for the study of protein molecular dynamics. There are many reasons for this which lie beyond the scope of the present discussion.

Despite a variety of experimental approaches and pulse sequences currently applied in NMR studies for obtaining information about molecular motions in different systems, all of them use only three natural NMR probes sensitive to molecular dynamics. One is the isotropic (i.e., averaged over all orientations) chemical shift of a magnetic nucleus. The chemical shift depends not only on the chemical structure of a macromolecule but also on its conformation. Suitable NMR experiments allow us to record the sensible change in chemical shift caused by molecular motions inherent in the mobile conformation of a biopolymer.

It is known that the chemical shift is a more or less anisotropic variable. In other words, the chemical shift depends on the orientation of the electron shell of a magnetic nucleus with respect to the external magnetic field $B_0$. This anisotropy is quantitatively characterized by the $3 \times 3$ tensor that (similar to the isotropic chemical shift) depends on the electronic structure of the molecule. Reorientation of the chemical shift anisotropy (CSA) tensor caused by molecular motions leads to a change in the chemical shift of the magnetic nucleus. The CSA tensor constitutes the second NMR probe sensitive to molecular dynamics. The electric field gradient of the quadrupole nuclei represents the same type of an NMR probe. These parameters provide information about purely rotational motions of magnetic nuclei.

Finally, the third probe responds to the dipole – dipole interaction between magnetic nuclei, governed by the distance between them and by the orientation of the internuclear vector with respect to the external magnetic field. Molecular motions are known to modulate both the internuclear distance (when the nuclei are not covalently bonded) and the orientation of the internuclear vector, thus influencing magnetic relaxation times.

Depending on whether a protein is in a solution or in the solid state, different types of experiments are conducted to study molecular mobility. Solution and solid state experiments yield information that differ considerably in terms of its type, precision, and variety. Solution experiments have an advantage in one case, and solid state studies in another. The main drawback of solid-state NMR experiments is their lower spectral resolution, which makes it difficult to assign spectral lines and obtain selective dynamic information. In solutions, the isotropic Brownian rotation of the protein molecule as a whole is superimposed on the internal dynamics, so that all slow internal motions with correlation time longer than that of Brownian rotation become practically 'invisible' for physical methods used to record the mechanical reorientation of one natural probe or another. Such methods include NMR relaxation, dielectric and fluorescent spectroscopies, and EPR. The correlation time of the Brownian rotation for the majority of proteins is on the order of $10^{-8}$ s; accordingly, all motions in the micro- and millisecond ranges become almost inaccessible for experimental studies. These motions in solutions can be examined only by such indirect methods as the hydrogen exchange technique or NMR methods that record chemical exchanges, i.e., modulation of the isotropic chemical shift by conformation transitions [11 – 13]. The main disadvantage of these approaches is that the magnitude of the chemical shift and the amplitude of its change depend on a large variety of structural and chemical properties of the macromolecule being investigated. Up to now, there have been no reliable algorithms for the computation of chemical shifts using structural data, let alone for the solution of the inverse problem. Therefore, an experimentally determined change in the chemical shift cannot in principle provide any information about the amplitude or geometric characteristics of slow molecular motions. Moreover, it is impossible to

determine by direct experiment what is actually in motion, the magnetic nucleus under observation or its immediate neighborhood (for example, the benzene ring of the closest aromatic group), which can also cause a change in the chemical shift. Although all these drawbacks are pretty obvious, the above experiments with protein solutions have been widely practiced in recent years for studying slow molecular motions, just because no better approaches are available.

Solid-state NMR spectroscopy provides many more opportunities for in-depth studies of the parameters of slow (i.e., in the micro- and millisecond ranges of correlation times) conformational dynamics. The set of NMR experiments suitable for the study of molecular dynamics in solid biopolymers has until recently been restricted to only two methods. One was the magnetic relaxation technique including relaxation in a rotating laboratory and dipole frame of reference, cross-relaxation between magnetic nuclei, and measurements of the linewidth in the NMR spectrum (or relaxation time $T_2$, which is the same). A combination of these relaxation techniques gives information about molecular motions in the correlation time range from $10^{-10}$ to $10^{-3}$ s. The second method consists in analyzing the line shape of the NMR spectrum of a sample, either static or slowly rotating at the magic angle (under the slow rotation condition is meant a rotational velocity lower than the CSA value expressed in frequency units). This method permits us to record any CSA tensor reorientation with a correlation time shorter than the characteristic time of the free induction decay (FID) or comparable to it. The frequency range of this method depends on magnetic nucleus CSA which is, in turn, determined by the type of nucleus and its electron shell. But most often line shape analysis is sensitive to molecular motions with correlation times of $10^{-4}$ s or less. NMR relaxation and line shape analysis are well-known standard methods for investigating molecular dynamics; their mathematical apparatus is described at length in a number of classical monographs concerning various aspects of magnetic resonance [14–16].

Molecular motions whose correlation times are longer than the FID time are possible to study only with the use of so-called exchange spectroscopy, the principles of which will be described at length below. Exchange spectroscopy has for a long time been successfully employed in liquid NMR spectroscopy, while its use in solid-state NMR spectroscopy was limited by a number of methodical problems, the most serious one being low sensitivity. However, modifications since the second half of the 1990s have allowed the efficacy of exchange NMR spectroscopy in solids to be substantially improved and the scope of its applications extended. This has made possible new original studies on the dynamic behavior of various solid-state molecular systems. The present review is designed to expound the principles of different types of exchange experiments and present examples of their use in biopolymer research.

## 2. Exchange experiment methods

To begin with, it is necessary to note that the term 'exchange' will be used here to define transition of a magnetic nucleus from a state with one chemical shift to a state with a different chemical shift. Such a transition can be induced either by a change in the isotropic chemical shift (i.e., local rearrangement of the chemical microenvironment of the nucleus) or by

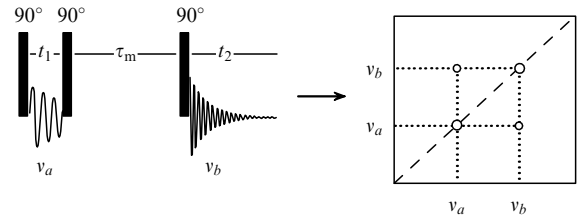


**Figure 1.** The simplest three-pulse sequence of a two-dimensional exchange NMR experiment (left) and the two-dimensional NMR spectrum (right).

reorientation of the CSA tensor. When the exchange characteristic time is longer than the FID time, this process has no effect on the shape of the NMR spectrum and can be revealed only with the use of special pulse sequences. Despite a variety of modifications to exchange NMR experiments, all variants of exchange pulse sequences always contain three functionally significant time periods. The first one is the period of evolution necessary to record the precession frequency of the magnetic nucleus, i.e., the magnitude of its chemical shift, at the initial moment. The second period is the mixing time during which the exchange act itself occurs. And last, the third period is the recording of the FID time during which the chemical shift is determined at the final moment. Although slow exchange is unapparent in a simple one-dimensional spectrum (see above), it can be seen in a two-dimensional one. The simplest pulse sequence of a two-dimensional exchange experiment first proposed in Ref. [17] is shown in Fig. 1.

The sequence consists of three 90°-pulses. One lays the magnetization vector on the plane $x-y$, thus making it precess with a circular frequency $\nu_a$. Another pulse returns the magnetization vector back toward the direction along the magnetic field $B_0$. The mixing period $\tau_m$ over, the third pulse again lays the magnetization vector on the plane $x-y$; afterwards, the recording of the FID time (i.e., precession frequency $\nu_b$) follows. This experiment results in $t_1$- and $t_2$-dependent two-dimensional free induction decay.

When the mixing time $\tau_m$ is much shorter than the correlation time $\tau_c$ of molecular motion, there is no exchange and $\nu_a$ equals $\nu_b$. In this case, the two-dimensional Fourier transform in variables $t_1$ and $t_2$ gives a two-dimensional spectrum with a simple one-dimensional spectrum residing the diagonal and no off-diagonal peaks being present. But if $\tau_m \geqslant \tau_c$ (and, accordingly, $\nu_a \neq \nu_b$), the two-dimensional spectrum shows off-diagonal peaks (cross peaks) symmetric with respect to the diagonal with the coordinates $(\nu_a, \nu_b)$ and $(\nu_b, \nu_a)$. By measuring the dependence of cross-peak amplitudes on the mixing time it is possible to extract information about the correlation time of molecular motion. In this case, the experiment becomes, strictly speaking, a three-dimensional one. It can be employed to record motions with a correlation time shorter than or comparable to the relaxation time $T_1$ due to the fact that the magnetization is oriented parallel to the field $B_0$ during the mixing period and therefore undergoes spin–lattice relaxation leading to the decay of the signal. The above sequence (see Fig. 1) is applicable to both solids and solutions, with the only difference that an exchange in solutions implies alteration of the isotropic chemical shift alone, because the overall CSA is averaged by rapid isotropic Brownian rotation, whereas in the solid state a change in both the isotropic chemical shift and the reorientation of the CSA tensor may occur.

It is important to note that cross peaks in a two-dimensional exchange spectrum may appear not only as a result of molecular and chemical exchange but also due to spin exchange. In solids, it is caused by spin diffusion, and in solutions by the Overhauser nuclear effect. In the latter case, the intensity of these cross peaks depends on the distance between magnetic nuclei, which makes it possible to apply exchange spectroscopy to the determination of spatial conformation of various molecules. Presently, NOESY (Nuclear Overhauser Effect SpectroscopY) experiment remains the main tool for the determination of the protein structure in solutions.

The application of the pulse sequence shown in Fig. 1 to the investigation of slow molecular dynamics in static isotropic solid samples has one important constraint. Dispersion of CSA tensor orientations leads to the dispersion of resonance frequencies $v_a$ and $v_b$ and to the appearance of the classical spectrum of a powder sample along the diagonal of the two-dimensional spectrum. In this case, the exchange manifests itself as a 'smearing out' of the spectrum off the diagonal and the appearance of intricately shaped reliefs rather than as a peculiarity in the form of isolated cross peaks [18]. Such a spectrum is open for quantitative analysis and can be used, in principle, for obtaining information about both the correlation times of molecular motions and their amplitudes (on the assumption that the exchange is due to the reorientation of the CSA tensor). However, such studies are of little practical value. First, line broadening associated with the dispersion of CSA tensor orientations results in low signal sensitivity. Second, this broadening makes it impossible to distinguish among various chemically nonequivalent (i.e., having different isotropic chemical shift) nuclei and, hence, to obtain selective information. For this reason, exchange experiments on solid samples are virtually inapplicable in this modification.

The standard method for line narrowing in solid-state NMR spectroscopy is the mechanical rotation of a sample about the magic angle, proposed by Raymond Andrew almost half a century ago [19]. Combined with the suppression of dipole–dipole internuclear interactions ('decoupling') during FID recording, the magic angle spinning (MAS) makes it possible to obtain NMR spectral line widths comparable to those in solutions. With these experimental techniques, the pulse sequence shown in Fig. 1 may be used to record chemical exchange (i.e., a change in isotropic chemical shift) in both solids and liquids in a similar way [20]. In the majority of cases, however, a change in the isotropic chemical shift in solids is very small compared with a change in the chemical shift produced by reorientation of the CSA tensor. Experimental examination of this reorientation is of great interest because it allows the amplitude of slow molecular motions to be determined. It should be recalled that such observations in solutions are impracticable in principle.

When recording rotational motion of the CSA tensor in an exchange experiment with MAS, one explicit condition must be fulfilled: the mixing time must be an integer multiple of the rotor rotation periods. It is necessary to have the sample similarly oriented immediately before and after the mixing time. Otherwise, it is impossible to distinguish between reorientations of the CSA tensor, caused by molecular motions and resulting from the mechanical rotation of the sample. In practice, this condition is realized by means of synchronization of the first and the third

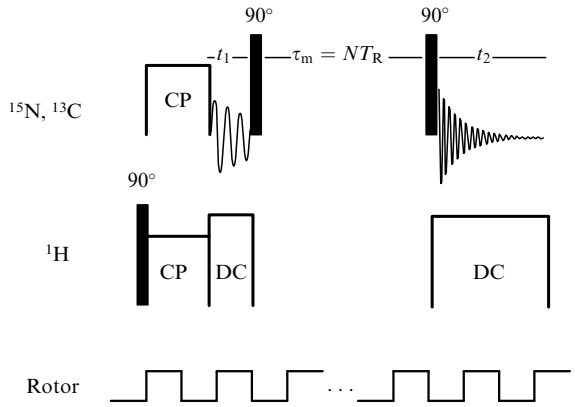


**Figure 2.** Pulse sequence of an exchange NMR experiment in solids with MAS; CP — cross-polarization, DC — decoupling, and $T_R$ — rotor rotation period.

90°-pulses with a varying signal from the system for stabilization of rotor rotations. The pulse sequence of such an experiment is presented in Fig. 2. Besides pulses acting on the nuclei under observation, it also shows those acting on protons. This is bound up with the fact that up till now the exchange experiments with proteins have been conducted only on $^{13}$C and $^{15}$N nuclei that are usually recorded by solid-state NMR spectroscopy with the use of standard cross-polarization [21] and decoupling techniques.

In order to understand how quantitative information about molecular dynamics can be extracted from a solid-state exchange experiment with MAS, one cannot do without a few mathematical expressions. A recent review [22] presented a rather detailed description of mathematical formalism of all currently known solid-state exchange experiments with the use of MAS. In what follows, we give the basic formulas that illustrate principles of quantitative analysis of solid-state exchange experiments and obtaining molecular dynamic information.

To begin with, there is a standard expression describing a free induction decay (FID) signal for an individual magnetic nucleus:

$$\mathrm{fid}\,(t) = M_0 \exp\left(\mathrm{i}\omega_0 t\right) \exp\left(-\frac{t}{T_2}\right), \tag{1}$$

where $M_0$ is equilibrium magnetization, $\omega_0$ is the circular resonance frequency, and $T_2$ is the transverse relaxation time. The resonance frequency of the magnetic nucleus is defined as

$$\omega_0 = \gamma B_0 \sigma_{zz}\,, \tag{2}$$

where $\gamma$ is the gyromagnetic ratio of the magnetic nucleus, $B_0$ is the constant external magnetic field, and $\sigma_{zz}$ is the $zz$-element of the CSA-tensor matrix on the assumption that the external magnetic field $B_0$ is directed along the $z$-axis. In the coordinate system of the principal CSA-tensor axes, i.e., in the system with zero off-diagonal elements, this tensor has the form

$$\boldsymbol{\sigma}^{\mathrm{PAS}} = \begin{pmatrix} \sigma_{11} & 0 & 0 \\ 0 & \sigma_{22} & 0 \\ 0 & 0 & \sigma_{33} \end{pmatrix}, \tag{3}$$

where the elements $\sigma_{11}$, $\sigma_{22}$, and $\sigma_{33}$ determine the chemical shift of the magnetic nucleus if the direction of $B_0$ coincides with axes $x$, $y$, and $z$ of this frame of reference, respectively (PAS — principal axes system). In order to pass from the principal axes system of the CSA tensor to the laboratory frame, the following standard transformation is used:

$$\boldsymbol{\sigma}^{\mathrm{LF}} = \mathbf{R}(\alpha,\beta,\gamma)\,\boldsymbol{\sigma}^{\mathrm{PAS}}\,\mathbf{R}^{-1}(\alpha,\beta,\gamma)\,, \tag{4}$$

where $\mathbf{R}(\alpha,\beta,\gamma)$ is the transition matrix from one coordinate system to another (LF — laboratory frame). The Euler angles $\alpha$, $\beta$, and $\gamma$ define successive rotations of the coordinate system during transition to the new system. Equation (4) being a standard procedure, we do not present here the explicit form of matrix $\mathbf{R}(\alpha,\beta,\gamma)$ and the exact definition of the Euler angles. If we deal with an isotropic sample — that is, an amorphous body, polycrystal, or powder, it is characterized by the uniform distribution of CSA tensors (hence, chemical shifts) over all possible orientations. In this case, it is necessary to integrate Eqn (1) over all orientations of the CSA tensor, i.e., over all Euler angles. This standard procedure, described in many NMR textbooks, leads to a static powder sample of a widely known form. From this form, it is possible to derive tensor elements $\sigma_{11}$, $\sigma_{22}$, and $\sigma_{33}$, and in the presence of molecular motions in the microsecond range one can evaluate their parameters. In the majority of cases, however, it is practically impossible to analyze the solid-state NMR spectrum of a static sample if it contains a few chemically nonequivalent nuclei and the dispersion of their isotropic chemical shifts is comparable to the CSA value.

When using MAS, equation (1) is modified; the resonance frequency acquires cyclic dependence on time: $\omega_0(t) = \omega_0(t + T_{\mathrm{R}})$, where $T_{\mathrm{R}}$ is the rotation period. Then, the free induction decay may be written in the following form

$$\mathrm{fid}\,(t) = M_0 \exp\left[\mathrm{i}\Theta(0,t)\right] \exp\left(-\frac{t}{T_2}\right), \tag{5}$$

where $\Theta(0,t)$ is the phase incursion of precessing magnetization by the time $t$:

$$\Theta(a,b) = \int_a^b \omega_0(t)\,\mathrm{d}t\,. \tag{6}$$

The resonance frequency $\omega_0$ is given by expression (2) in which the $zz$-element of the CSA tensor assumes time dependence. It can be shown that

$$\omega_0(t) = \omega_{\mathrm{L}}\sigma_{\mathrm{iso}} + \omega_{\mathrm{L}}\sigma_{\mathrm{aniso}}^{\mathrm{LF}}(t) = \omega_{\mathrm{iso}} + \omega_{\mathrm{aniso}}(t)\,, \tag{7}$$

where $\omega_{\mathrm{L}}$ is the Larmor frequency of the magnetic nucleus, $\sigma_{\mathrm{iso}}$ and $\sigma_{\mathrm{aniso}}$ denote isotropic and anisotropic constituents of the chemical shift:

$$\sigma_{\mathrm{iso}} = \frac{1}{3}(\sigma_{11} + \sigma_{22} + \sigma_{33})\,, \tag{8}$$

$$\begin{aligned}\sigma_{\mathrm{aniso}}(t) = {} & C_2\cos(2\omega_{\mathrm{R}}t + 2\gamma) + S_2\sin(2\omega_{\mathrm{R}}t + 2\gamma) \\ & + C_1\cos(\omega_{\mathrm{R}}t + \gamma) + S_1\sin(\omega_{\mathrm{R}}t + \gamma)\,;\end{aligned} \tag{9}$$

(here, $\omega_{\mathrm{R}}$ is the MAS circular frequency), and coefficients $C_{1,2}$ and $S_{1,2}$ are expressed as

$$\begin{aligned}C_2 = \frac{1}{3}\Bigg\{ & \frac{3}{2}(\sigma_{33} - \sigma_{\mathrm{iso}})\sin^2\beta \\ & - \frac{1}{2}\left[\frac{1}{2}(\sigma_{22} - \sigma_{11})\cos 2\alpha - \sigma_{12}\sin 2\alpha\right](3 + \cos 2\beta) \\ & - (\sigma_{13}\cos\alpha + \sigma_{23}\sin\alpha)\sin 2\beta\Bigg\}\,,\end{aligned} \tag{10a}$$

$$\begin{aligned}S_2 = \frac{2}{3}\Bigg\{ & \left[\frac{1}{2}(\sigma_{22} - \sigma_{11})\sin 2\alpha + \sigma_{12}\cos 2\alpha\right]\cos\beta \\ & + (\sigma_{13}\sin\alpha - \sigma_{23}\cos\alpha)\sin\beta\Bigg\}\,,\end{aligned} \tag{10b}$$

$$\begin{aligned}C_1 = \frac{\sqrt{2}}{3}\Bigg\{ & -\frac{3}{2}(\sigma_{33} - \sigma_{\mathrm{iso}})\sin 2\beta \\ & - \left[\frac{1}{2}(\sigma_{22} - \sigma_{11})\cos 2\alpha - \sigma_{12}\sin 2\alpha\right]\sin 2\beta \\ & + 2(\sigma_{13}\cos\alpha + \sigma_{23}\sin\alpha)\cos 2\beta\Bigg\}\,,\end{aligned} \tag{10c}$$

$$\begin{aligned}S_1 = \frac{2\sqrt{2}}{3}\Bigg\{ & \left[\frac{1}{2}(\sigma_{22} - \sigma_{11})\sin 2\alpha + \sigma_{12}\cos 2\alpha\right]\sin\beta \\ & - (\sigma_{13}\sin\alpha - \sigma_{23}\cos\alpha)\cos\beta\Bigg\}\,.\end{aligned} \tag{10d}$$

The Euler angles $\alpha$, $\beta$, and $\gamma$ in Eqns (9) and (10) denote the transition from the rotor frame of reference, in which the $Z$-axis is oriented along the rotor rotation axis, to the molecular frame of reference. CSA tensor elements $\sigma$ in Eqns (10) correspond to its representation in this molecular frame of reference, which can, in principle, have arbitrary orientation. It is not quite correct to relate the molecular frame of reference to the principal axis system of the CSA tensor; in what follows, we shall consider motions of the CSA tensor just with respect to the molecular frame of reference. Furthermore, integration in Eqn (6) taking into account Eqns (7)–(10) yields

$$\begin{aligned}\mathrm{fid}\,(t) = {} & \exp(\mathrm{i}\omega_{\mathrm{iso}}t)\exp\left[-\mathrm{i}\Psi(\gamma)\right] \\ & \times \exp\left[\mathrm{i}\Psi(\gamma + \omega_{\mathrm{R}}t)\right]\exp\left(-\frac{t}{T_2}\right),\end{aligned} \tag{11a}$$

where

$$\Psi(x) = \frac{\omega_{\mathrm{L}}}{\omega_{\mathrm{R}}}\left(\frac{C_2}{2}\sin 2x - \frac{S_2}{2}\cos 2x + C_1\sin x - S_1\cos x\right). \tag{12}$$

By introducing notation

$$f(x) = \exp\left[\mathrm{i}\Psi(x)\right], \tag{13}$$

equation (11a) can be rewritten in the form

$$\mathrm{fid}\,(t) = \exp(\mathrm{i}\omega_{\mathrm{iso}}t)\,f^*(\gamma)\,f(\gamma + \omega_{\mathrm{R}}t)\exp\left(-\frac{t}{T_2}\right); \tag{11b}$$

$f(x)$ is the so-called $f$-function determining the phase correlation of transverse magnetization.

Passing to an isotropic sample, i.e., performing the integration over the Euler angles $\alpha$, $\beta$, and $\gamma$, leads to the following expression for FID:

$$\mathrm{fid}\,(t) = \exp\left(\mathrm{i}\omega_{\mathrm{iso}}t\right)\exp\left(-\frac{t}{T_2}\right)\sum_{N=-\infty}^{\infty}\exp\left(\mathrm{i}N\omega_{\mathrm{R}}t\right)I_N\,, \quad (14)$$

where

$$I_N = \frac{1}{4\pi}\int_0^{2\pi}\mathrm{d}\alpha\int_0^{\pi}\sin\left(\beta\right)F_N^{*}F_N\,\mathrm{d}\beta\,, \quad (15)$$

$$F_N = \frac{1}{2\pi}\int_0^{2\pi}\exp\left(-\mathrm{i}Nx\right)f(x)\,\mathrm{d}x\,. \quad (16)$$

Expression (14) gives a good idea of the shape of the NMR spectrum of a sample rotating at the magic angle: it consists of isolated narrow peaks separated by a frequency interval $\omega_{\mathrm{R}}$. In the literature, these peaks are often termed the spinning side bands (ssb). The central peak corresponding to $N = 0$ lies at the frequency of the isotropic chemical shift. Intensities of these peaks are proportional to $I_N$.

Using the notions and notations introduced in the foregoing discussion, we may move to the quantitative description of a two-dimensional exchange experiment whose pulse sequence is depicted in Fig. 2. To begin with, let us assume that the molecular motion consists in hopping the CSA tensor from one orientation relative to the molecular frame of reference to another. Each orientation is defined by its own Euler angles that specify the transition matrix from the molecular frame of reference to the coordinate system of principal axes of the CSA tensor. A model of quick hops between discrete positions (orientations) is also applicable to approximating the diffuse continuous rotation of the CSA tensor. It can be achieved by a simple increase in the number of possible orientations of the CSA tensor. The transition probability from one orientation to another per unit time is given by the so-called exchange matrix **K**. The off-diagonal element $K_{ji}$ $(j \neq i)$ of this matrix determines the hopping probability per unit time from orientation $i$ to orientation $j$, while the diagonal element $K_{jj}$ determines the probability of transition from state $j$ to all other orientations with a negative sign. In other words, the model of motion is formally given by (1) the number of possible orientations of the CSA tensor (hereinafter denoted as $N_S$), (2) the set of Euler angles for each orientation, and (3) the exchange matrix. Let us now see how it is reflected in an exchange experiment.

By the end of the evolution period (time $t_1$), the transverse magnetization of magnetic nuclei having the CSA tensor in orientation $j$ is expressed as

$$\mathrm{fid}^{\,j}\,(t_1) = P_j^{\mathrm{eq}}\exp\left[\mathrm{i}\Theta^j(0,t_1)\right]\exp\left(-\frac{t_1}{T_2}\right), \quad (17)$$

where $\Theta^j(0,t_1)$ is given by Eqn (6), and $P_j^{\mathrm{eq}}$ is the equilibrium population of orientation $j$ that is, in turn, determined by the Boltzmann distribution. Let us assume that during the mixing time part of the CSA tensors has passed from orientation $j$ to orientation $i$ in the course of molecular motion. For these tensors, transverse magnetization by the end of period $t_2$ will be expressed as

$$\mathrm{fid}^{\,ij}\,(t_1,\tau_{\mathrm{m}},t_2) = Q_{ij}(\tau_{\mathrm{m}})\exp\left[\mathrm{i}\Theta^j(0,t_1)\right] \times\exp\left[\mathrm{i}\Theta^i(t_1+\tau_{\mathrm{m}},\,t_1+\tau_{\mathrm{m}}+t_2)\right]\exp\left(-\frac{t_1+t_2}{T_2}\right), \quad (18)$$

where

$$Q_{ij}(\tau_{\mathrm{m}}) = P_{ij}(\tau_{\mathrm{m}})\,P_j^{\mathrm{eq}}\exp\left(-\frac{\tau_{\mathrm{m}}}{T_1}\right). \quad (19)$$

In equation (19), $P_{ij}(\tau_{\mathrm{m}})$ defines the probability of transition of the CSA tensor from orientation $j$ to orientation $i$ for time $\tau_{\mathrm{m}}$. These probabilities can be found from the differential matrix equation

$$\frac{\mathrm{d}\overline{P(t)}}{\mathrm{d}t} = \mathbf{K}\overline{P(t)}\,, \quad (20)$$

where **K** is the exchange matrix. The solution of Eqn (20) is reduced to the standard form

$$\overline{P(t)} = \exp\left(\mathbf{K}t\right)\overline{P(0)}\,, \quad (21)$$

whence it can be seen that probabilities $P_{ij}(\tau_{\mathrm{m}})$ are defined as

$$P_{ij}(\tau_{\mathrm{m}}) = \left(\exp\left(\mathbf{K}\tau_{\mathrm{m}}\right)\right)_{ij}. \quad (22)$$

The exponential matrix in Eqn (22) takes the following explicit form

$$\exp\left(\mathbf{K}\tau_{\mathrm{m}}\right) = \mathbf{R}_{\mathrm{D}}\begin{bmatrix}\exp\left(K_1\tau_{\mathrm{m}}\right) & 0 & \ldots & 0\\ 0 & \exp\left(K_2\tau_{\mathrm{m}}\right) & \ldots & 0\\ \ldots & \ldots & \ldots & \ldots\\ 0 & 0 & \ldots & \exp\left(K_{N_S}\tau_{\mathrm{m}}\right)\end{bmatrix}\mathbf{R}_{\mathrm{D}}^{-1}\,, \quad (23)$$

where $K_1, K_2, \ldots, K_{N_S}$ are the eigenvalues of the matrix **K**, and $\mathbf{R}_{\mathrm{D}}$ is the transformation matrix bringing **K** to the diagonal form.

Recalling the definition of the $f$-function and that the mixing time is an integer multiple of rotor periods, Eqn (18) can be rewritten in the following form

$$\mathrm{fid}^{\,ij}\,(t_1,\tau_{\mathrm{m}},t_2) = Q_{ij}(\tau_{\mathrm{m}})\exp\left(-\frac{t_1+t_2}{T_2}\right)\exp\left(\mathrm{i}\omega_{\mathrm{iso}}^{j}t_1\right) \times\exp\left(\mathrm{i}\omega_{\mathrm{iso}}^{i}t_2\right)f^{j*}(\gamma)\,f^{j}(\gamma+\omega_{\mathrm{R}}t_1)\,f^{i*}(\gamma+\omega_{\mathrm{R}}t_1) \times f^{i}(\gamma+\omega_{\mathrm{R}}t_1+\omega_{\mathrm{R}}t_2)\,. \quad (24)$$

Superscripts $i$ and $j$ on $f$-functions indicate that they correspond to orientations $i$ and $j$ of the CSA tensor and have different coefficients $C_1$, $C_2$, $S_1$, and $S_2$ [formulas (10)] which determine the $f$-function. Integrating this expression over the Euler angles $\alpha$, $\beta$, and $\gamma$, i.e., moving to an isotropic sample, one obtains

$$\mathrm{fid}^{\,ij}\,(t_1,\tau_{\mathrm{m}},t_2) = Q_{ij}(\tau_{\mathrm{m}})\exp\left(-\frac{t_1+t_2}{T_2}\right)\exp\left(\mathrm{i}\omega_{\mathrm{iso}}^{j}t_1\right) \times\exp\left(\mathrm{i}\omega_{\mathrm{iso}}^{i}t_2\right)\sum_{M,N}\exp\left(\mathrm{i}M\omega_{\mathrm{R}}t_1\right)\exp\left(\mathrm{i}N\omega_{\mathrm{R}}t_2\right)I_{MN}^{ij}\,, \quad (25)$$

where

$$I_{NM}^{ij} = \frac{1}{4\pi}\int_0^{2\pi}\int_0^{\pi}F_M^{j}\,F_{M-N}^{ij}\,F_N^{i*}\sin\beta\,\mathrm{d}\beta\,\mathrm{d}\alpha\,; \quad (26)$$

here, the coefficients $F_M^i$ are given by Eqn (16), and $F_{M-N}^{ij}$ looks like

$$F_{M-N}^{ij} = \frac{1}{2\pi}\int_0^{2\pi}\exp\left[-\mathrm{i}(M-N)x\right]f^{j}(x)\,f^{i*}(x)\,\mathrm{d}x\,. \quad (27)$$

It follows from Eqn (25) that the cross-peak amplitude in the two-dimensional spectrum at a point with coordinates $(\omega_{iso} + M\omega_R, \omega_{iso} + N\omega_R)$ (without regard for spin–lattice relaxation), corresponding to the nuclei whose CSA tensors were in orientation $j$ before the mixing time and orientation $i$ after it (or vice versa, which is the same), is defined by the quantity $I_{MN}^{ij}$. Peaks corresponding to the one-dimensional spectrum with MAS are located along the diagonal (i.e., under condition $N = M$). The total intensity of the peaks in the two-dimensional spectrum is found by summation over all orientations prior to and after the mixing period:

$$\mathrm{INT}_{NM}(\tau_m) = \sum_{i,j}^{N_S} Q_{ij}(\tau_m)\, I_{NM}^{ij}\,. \tag{28}$$

It is easy to show that in the simplest case of exchange between two equally probable orientations of the CSA tensor the dependence of cross-peak intensity on mixing time is determined by the following expression

$$\mathrm{INT}_{NM}(\tau_m) = \left[1 - \exp\left(-2k\tau_m\right)\right] \frac{I_{NM}^{11} + I_{NM}^{12}}{2} \exp\left(-\frac{\tau_m}{T_1}\right), \tag{29}$$

where $k$ is the exchange rate between orientations 1 and 2, incorporated in the exchange matrix.

It is appropriate here to make four notes on the properties and nature of an exchange experiment with MAS. First, the cross-peak amplitude is obviously determined by the geometric parameters of the molecular motion. In the first approximation, it can be said that the smaller the angular amplitude of the CSA tensor orientation, the lower the cross-peak amplitude. In the limiting case, when the two orientations coincide, $f^j(x) = f^i(x)$ in formula (27). It can then be shown that the sum in Eqn (25) becomes proportional to the delta-function with argument $M-N$, whence it follows that in this case the spectrum displays only peaks for which $M = N$, i.e., diagonal ones, and there are no off-diagonal peaks. This dependence of the cross-peak amplitude on CSA-tensor reorientation geometry makes it possible to obtain information not only about the frequency parameters of molecular dynamics, but also about the amplitude parameters.

Second, it is obvious from the definition of function $\Psi(x)$ (12), which in its turn determines $f$-function (13), that the cross-peak amplitude depends on both the resonance frequency $\omega_L$ and the MAS frequency $\omega_R$. This means that in order to obtain the maximum cross-peak intensity relative to the central diagonal peak, it is necessary to employ the maximally attainable resonance frequency and rotate the sample as slowly as possible. The choice of the resonance frequency in this situation is determined only by the available set of NMR spectrometers and, alas, is rarely as wide as the researcher would wish to use. Also, the MAS rate must be chosen by taking into account the possibility of high spectral resolution and as high a signal-to noise ratio as possible; in other words, the choice of $\omega_R$ is always a matter of compromise.

Third, a two-dimensional exchange experiment allows one to observe both CSA tensor orientation (which was the main topic of the foregoing discussion) and chemical exchange processes, i.e., a change in the isotropic chemical shift. It is seen from Eqn (25) that the appearance of cross peaks may result not only in different CSA tensor orientations but also in a change in the isotropic chemical shift. It is for this reason that the frequencies $\omega_{iso}^i$ and $\omega_{iso}^j$ in equation (25) can be different in the general case. However, as mentioned above, a change in the isotropic chemical shift in biopolymers, caused by conformational dynamics, is very often negligibly small compared to a change in the chemical shift attributable to CSA tensor reorientation.

The fourth note concerns spin diffusion. As mentioned above, spin diffusion may give rise to cross peaks even in the absence of molecular motions. Strictly speaking, an exchange experiment by itself does not allow one to distinguish between CSA tensor reorientation (or a change in the isotropic chemical shift) and magnetization diffusion (the so-called flip-flop process) from one magnetic nucleus to another. Despite the obvious difference in the physical nature of these processes, their manifestation in an exchange experiment and the above mathematical description are absolutely identical. The sole clue to direct the experimenter is the measurement of the temperature dependence of the exchange time. The correlation time of molecular mobility depends on temperature, whereas the spin diffusion rate practically does not because it is only determined by the system of internuclear distances in a given sample. This discrepancy may be of use for discriminating between these two effects.

For all the numerous advantages of the two-dimensional exchange experiment with MAS described above, it has an important drawback: in many cases it requires time-consuming measurements. Recording a two-dimensional spectrum only at one mixing time takes at least one hour but more frequently a few hours and even days. When the aim is to obtain information about the correlation time of slow motion, experiments have to be carried out at several mixing times, and their total duration increases accordingly. When temperature dependences need to be determined in addition, the time of the study of a single sample most commonly extends beyond a reasonable limit. This accounts for the fact that a two-dimensional exchange NMR spectroscopy of solids is not employed as extensively as it might be. At least to our knowledge, there is not a single example of its application to the investigation into the molecular dynamics of biological polymers.

A solution to this problem, even if partial, turned out to be a decrease in the dimensionality of the exchange experiment: from two-dimensional to one-dimensional, which allows its duration to be reduced almost by one order of magnitude without the loss of quality and quantity of dynamic information. The development of one-dimensional modifications of the solid-state exchange NMR experiment with MAS dates to the mid-1990s. The main idea underlying the passage from a two-dimensional exchange experiment to its one-dimensional modification consists in fixing time $t_1$ at a certain value related to the MAS frequency and in using special phase cycling of radiofrequency pulses appearing in the sequence. The exchange process in a two-dimensional experiment is recognized by the presence of off-diagonal peaks in the two-dimensional spectrum, whereas in the one-dimensional modifications, the exchange can be recorded only by measuring the mixing time dependence of spectral line amplitudes (intensities). In the absence of exchange, a decrease in the spectral amplitude is only determined by

spin-lattice relaxation. Otherwise, the amplitude decreases much faster. Both the magnitude and the characteristic time of this additional fall are determined by the parameters of exchange process.

Thus far, a few one-dimensional solid-state NMR experiments with MAS have been proposed:

— ODESSA (One-Dimensional Exchange Spectroscopy of Ssb Alternation) [23];

— tr-ODESSA (time-reverse ODESSA) [24];

— Seldom ODESSA (SELectivity by Destruction Of Magnetization) [25];

— EIS (Exchange Induced Ssb) [26];

— PATROSS (Phase Adjusted ssb TR-OdeSSa) [27], and

— CODEX (Centerband-Only Detection of EXchange) [28, 29].

It is worth noting, without going into the methodical details of each of these experiments, that the most practicable and convenient of them is the CODEX pulse sequence. The main methodical problem of exchange experiments is the choice of the MAS frequency. As mentioned earlier, on the one hand it must be as low as possible to have the effect of the exchange maximally apparent. On the other hand, it must be sufficiently high to ensure good spectral resolution and maximum signal-to-noise ratio. This contradiction is best resolved in the CODEX experiment; therefore, only this type of one-dimensional exchange experiment has been used since 2000 to study the slow dynamics of both synthetic and biological polymers. As concerns the latter, the tr-ODESSA sequence was also used, besides the CODEX sequence, in one study [30] to follow protein dynamics. This work will be considered below.

Pulse sequences of the tr-ODESSA and CODEX experiments are presented in Figs 3 and 4. In the tr-ODESSA sequence, time $t_1$ is always equal to the MAS half-period, mixing time is invariably an odd number of MAS half-periods, and free induction signals begin to be recorded after the half-period of MAS following the last 90°-pulse. An important role in this experiment is played by the phase cycle of the pulses and of the free-induction-signal detection frequency, as described at length in Ref. [24]. Due to this phase cycle, central and ssb peaks of all chemically nonequivalent magnetic nuclei have positive amplitudes at any mixing time, regardless of the presence or absence of exchange. In a previous version of this experiment [23], the amplitudes of the central and ssb peaks varied according to

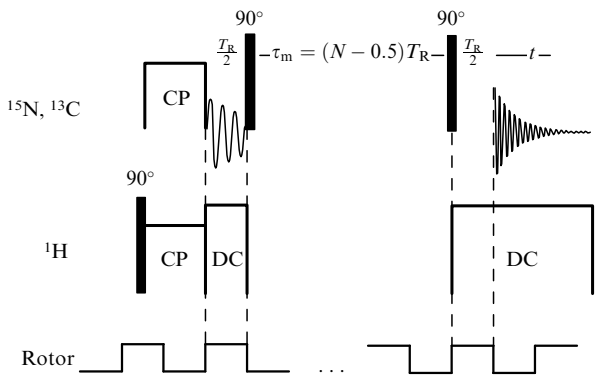


**Figure 3.** Pulse sequence of one-dimensional solid-state exchange NMR experiment tr-ODESSA [24].

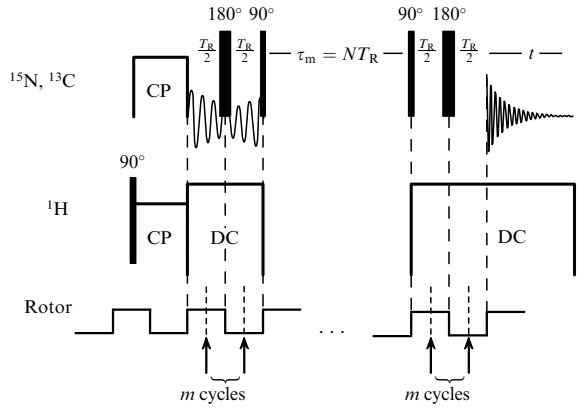


**Figure 4.** Pulse sequence of one-dimensional solid-state exchange NMR experiment CODEX [28, 29].

the law $(-1)^N$, where $N$ is the serial number of the ssb peak ($N = 0$ corresponds to the central peak). In the presence of several nonequivalent nuclei in a molecule, this may substantially complicate the shape of the NMR spectrum, as well as the molecular dynamic analysis.

Eventually, the intensity of the central and ssb peaks is defined as

$$I_N^{\text{trODESSA}} = \sum_{i,j}^{N_S} \sum_M Q_{ij}(\tau_m)(-1)^{M-N} I_{NM}^{ij}\,, \tag{30}$$

where notations $Q_{ij}(\tau_m)$, $M$, $N$, and $I_{NM}^{ij}$ play the same role as in the two-dimensional exchange experiments discussed in a previous paragraph. Thus, in the tr-ODESSA experiment, the peak in a one-dimensional spectrum is the sum of the peak of the simple one-dimensional spectrum and all the cross peaks of the spectrum of the two-dimensional exchange experiment, located along one vertical (or, which is the same, horizontal) line with alternating signs.

The main feature of the CODEX pulse sequence (see Fig. 4) is that the spins are affected before and after the mixing time by a cycle of $m$ 180°-pulses ($m$ being strictly an odd number) separated by the MAS half-period. Therefore, the period of evolution may consist of a few MAS periods. The physical meaning of these pulses lies in the fact that they cause the CSA reinversion every MAS half-period and thus preclude averaging CSA even at a very rapid MAS. Their action is in a way analogous to that of 180°-pulses in the well-known Carr – Purcell sequence where they compensate for the effect of magnetic field inhomogeneity. In the case being considered, 180°-pulses compensate for the MAS effect due to a change in the sign of the precessing magnetization phase every MAS half-period. As a result, there is no averaging of CSA in the periods prior to and after the mixing time. This provides information about the CSA tensor reorientation; at the same time, the NMR spectrum has more intense central peaks due to the rapid MAS, which improves both the signal-to-noise ratio and the spectral resolution.

The intensity of spectral lines in the CODEX experiment is expressed in a somewhat more complicated form

$$I_N^{\text{CODEX}} = \sum_{i,j}^{N_S} Q_{ij}(\tau_m)\, I_N^{ij,\,\text{CODEX}}\,, \tag{31}$$

where

$$I_N^{ij,\,\mathrm{CODEX}} = \frac{1}{4\pi}\int_0^{2\pi}\int_0^{\pi} C_N^{ij}(\alpha,\beta)\sin\beta\,\mathrm{d}\beta\,\mathrm{d}\alpha\,, \tag{32}$$

$$\begin{aligned} C_N^{ij}(\alpha,\beta) = {} & \sum_M \exp\left[\mathrm{i}(M-N)\pi\right] \\ & \times\left[\frac{1}{2\pi}\int_0^{2\pi}\exp\left(\mathrm{i}M\gamma\right) f^{i*}(\gamma)\left(f^{j*}(\gamma)f^{i}(\gamma)\right)^{m+1}\mathrm{d}\gamma\right] \\ & \times\left[\frac{1}{2\pi}\int_0^{2\pi}\exp\left[-\mathrm{i}(M-N)\vartheta\right]\left(f^{j}(\vartheta)f^{i*}(\vartheta)\right)^{m+1}\mathrm{d}\vartheta\right] \\ & \times\left[\frac{1}{2\pi}\int_0^{2\pi}\exp\left(-\mathrm{i}N\phi\right) f^{i}(\phi)\,\mathrm{d}\phi\right]. \end{aligned} \tag{33}$$

It follows from these formulas that the larger $m$, the higher the sensitivity of the experiment to the exchange (i.e., the stronger the dependence of the peak amplitude on the mixing time). In a tr-ODESSA experiment, a similar rise can be achieved only by decreasing the MAS frequency, which leads (as mentioned above) to a diminished signal-to-noise ratio and the deterioration of the spectral resolution. At the same time, a rise in the MAS frequency and $m$ in a CODEX experiment also has a natural limit: the length of the 180°-pulse at high MAS rates becomes comparable to the rotation period, which markedly complicates the quantitative analysis of the data obtained. Moreover, it should be borne in mind that prolongation of the evolution period, i.e., increasing the product $mT_{\mathrm{R}}$, may result in a substantially worsened signal-to-noise ratio, when $mT_{\mathrm{R}}$ is close to $T_2$. One more peculiarity of this experiment lies in the fact that it is insensitive to chemical change (i.e., to a change in the isotropic chemical shift), unlike tr-ODESSA, and reflects only reorientation of the CSA tensor. This can be accounted for by the presence of 180°-pulses that level differences between magnetization precession rates before and after the mixing time that arises as a consequence of the difference between the isotropic chemical shifts. This is a well-known property of the Carr–Purcell sequence.

The above-presented mathematical formalism of exchange experiments with MAS can be reduced to one schematic expression

$$\text{Line amplitude} = \text{Function}\left(\begin{array}{cc} \text{Experimental parameters:} & \text{Molecular parameters:} \\ \omega_{\mathrm{L}}\text{ — resonance frequency} & \boldsymbol{\sigma}\text{ — CSA tensor} \\ \omega_{\mathrm{R}}\text{ — MAS frequency} & N_S\text{ — number of possible orientations} \\ t_1\text{ — evolution period} & \text{of the CSA tensor} \\ \tau_{\mathrm{m}}\text{ — mixing time} & \alpha_i,\beta_i,\gamma_i,\ i=1,N_S\text{ — Euler angles for all orientations} \\ & \mathbf{K}\text{ — exchange matrix} \end{array}\right). \tag{34}$$

Meaning of the exchange experiments lies in the fact that by measuring the line amplitude in an NMR spectrum under different experimental conditions, most of all at different mixing times, we can determine the molecular dynamic parameters with the aid of scheme (34). Certainly, the concrete form of the Function in expression (34) depends on the type of exchange experiment. The time range of molecular motions, to which exchange experiments are susceptible, is determined, on the one hand, by the minimal mixing time, and by the relaxation time $T_1$, on the other hand. Because the minimal mixing time depends on the MAS period, it may be as small as fractions of a millisecond (typical values of the MAS rate are a few kilohertz). As for the time $T_1$, it depends on many parameters, both experimental and molecular, and can vary from dozens and hundreds of milliseconds to dozens and hundreds of seconds.

To conclude the methodical section of this review, a few notes are in order concerning magnetic nuclei with which it is possible to conduct exchange NMR experiments. All NMR experiments on proteins, except for a few studies, have until recently been carried out with only four types of nuclei, viz. $^1$H, $^2$H, $^{13}$C, and $^{15}$N. Experiments with protons and carbon-13 nuclei can be performed at their natural abundance in a sample, whereas studies using deuterons and nitrogen-15 nuclei require either complete or selective enrichment of the samples. Nuclei having maximum CSA are the most convenient for conducting solid-state exchange experiments due to the higher amplitude of exchange decay in the mixing time dependence of spectral line intensities. For this reason, protons are almost totally unsuitable for exchange experiments, their CSA in organic compounds being very small and the time $T_2$ so short that FID practically vanishes in the course of evolution. The remaining three types of magnetic nuclei are quite suitable for exchange experiments, although to a different extent. Deuterons have the highest degree of CSA (of quadrupole splitting anisotropy, to be more precise), but at the same time the shortest $T_1$, which accounts for narrowing the time range of sensitivity of an exchange experiment. Moreover, deuterons are characterized by the very narrow limits of scatter in isotropic chemical shifts, which makes it impossible to resolve and assign the lines of complex spectra. That is why deuterons are frequently used to label only one chemical site in a protein. This solves the problem of assignment of spectral lines but worsens the representativeness of the information obtained in NMR experiments. Up to now, deuterons have not been used in solid-state exchange NMR studies of protein dynamics, even though they have been extensively employed in the analysis of the spectral line shape of static samples [31]. The largest degree of CSA is inherent in those $^{13}$C and $^{15}$N nuclei that are located in the backbone chain. First and foremost, these are carbonyl carbons and nitrogens covalently bonded to them; alpha-carbons are less frequently used for the purpose. Aliphatic carbons and nitrogens localized at side chains have a much lower degree of CSA although these nuclei can also be used, in principle, for an exchange experiment provided there is good signal sensitivity, high resonance frequency, and a large number of accumulations. Certainly, each concrete experiment involves specific factors that make selected magnetic nuclei either convenient and reasonable or impracticable to use for one purpose or another. As a general rule, it may be stated that the concurrent employment of different magnetic nuclei in one and the same sample permits us to substantially increase the amount and improve the precision of molecular dynamic information. Alas, this goal is frequently unattainable for technical reasons.

## 3. Application of solid-state exchange experiments in protein dynamics studies

The first report on protein dynamics studies by the solid-state exchange NMR technique was published in 1999 [30]. This

investigation was designed to elucidate the backbone dynamics of the barstar protein and a synthetic polypeptide, polyglycine. Barstar experiments were carried out on $^{15}$N nuclei; for this purpose, the protein was fully enriched with the isotope $^{15}$N. In experiments with polyglycine, $^{13}$C nuclei were used at their natural abundance in the samples. The experiments were based on the tr-ODESSA pulse sequence [24]. Similar to many other works on protein dynamics in the solid state, the researchers investigated barstar and polyglycine in both dry and wet conditions. The interest in experiments under different hydration conditions arises from the fact that the interaction of protein with water determines many of its functional properties, including internal dynamics (see reviews [32, 33]). Using different levels of moisture allowed experimenters to study the character and the nature of hydrate water effects on the selected characteristics of a given protein. Total enrichment in $^{15}$N nuclei produced in the one-dimensional solid-state spectrum one broad line corresponding to backbone nitrogens and thus provided only integrated information about the averaged dynamic behavior of the entire backbone chain. As for polyglycine, it showed two spectral lines corresponding to carbonyl carbons and alpha-carbons. The work being considered analyzed the amplitude of the carbonyl lines because they possessed a much higher degree of CSA. Separate measurements of the relaxation time $T_1$ were conducted by the standard method [34] in order to take into account spin – lattice relaxation. Thereafter, the ratio of the line amplitude in the exchange experiment to the amplitude of the same line in the relaxation experiment was calculated at the identical mixing time and relaxation delay in these two experiments, respectively. This standard exchange decay correction procedure permitted us to exclude the spin – lattice relaxation effect.

Both barstar and polyglycine exhibited exchange decay of a rather high amplitude with the characteristic time on the order of hundreds of milliseconds. However, it appeared from temperature dependences that this decay was largely caused by spin diffusion between magnetic nuclei rather than by molecular motions. This inference ensues from the analysis of temperature dependences of exchange decays that was performed in this work for a range between $-50\,^{\circ}$C and $+100\,^{\circ}$C. Only barstar containing up to 0.2 g of water per 1 g of protein at temperatures above $0\,^{\circ}$C showed the temperature dependence of the shape of the initial portion of exchange decay (first 300 – 400 ms). In no other cases did barstar as well as dry or wet polyglycine exhibit any temperature dependence of the shape of the exchange decay. From this follows that molecular motions of the backbone chain are manifested only in wet barstar, whereas the structures of dry barstar and polyglycine are too rigid for such slow and large-scale conformational motions to occur.

In order to explain why the molecular motions fail to manifest themselves in wet barstar at low temperatures, the exchange model shown in Fig. 5 was analyzed quantitatively. It suggests the participation of two magnetic nuclei in the hops between two equally probable orientations — that is, between orientations 1 and 2 for one nucleus, and between orientations 3 and 4 for the other nucleus. It is assumed for simplicity that the two nuclei possess identical parameters of the molecular motion. At the same time, spin exchange occurs between the two nuclei. Exchange pathways between the four positions are shown by arrows in Fig. 5. The molecular reorientation rate is denoted by $k_{MR}$, and the spin exchange

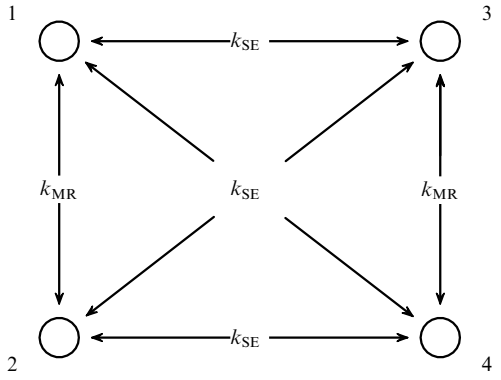


**Figure 5.** Schematic of spin exchange between two magnetic nuclei that in their turn participate in molecular motions or hops between two equally probable positions.

rate by $k_{SE}$. The exchange matrix for such a system looks like

$$\mathbf{K} = \begin{pmatrix} -2k_{SE}-k_{MR} & k_{MR} & k_{SE} & k_{SE} \\ k_{MR} & -2k_{SE}-k_{MR} & k_{SE} & k_{SE} \\ k_{SE} & k_{SE} & -2k_{SE}-k_{MR} & k_{MR} \\ k_{SE} & k_{SE} & k_{MR} & -2k_{SE}-k_{MR} \end{pmatrix}. \tag{35}$$

Calculations using this matrix, as described above, on the assumption that $I_N^{13} = I_N^{14} = I_N^{23} = I_N^{24}$ and $I_N^{12} = I_N^{34}$ (where $I_N^{ij}$ is the intensity of the ssb peak with ordinal number $N$ in the tr-ODESSA experiment (30) at a zero mixing time) give the following dependence of line intensity on the mixing time:

$$\frac{I_N(\tau_m)}{I_N(0)} = \left[1 - P_1\left(1 - \exp\left(-\frac{\tau_m}{\tau_1}\right)\right) - P_2\left(1 - \exp\left(-\frac{\tau_m}{\tau_2}\right)\right)\right] \exp\left(-\frac{\tau_m}{T_1}\right), \tag{36}$$

where

$$I_N(0) = I_N^{11}, \quad P_1 = \frac{I_N^{11} - I_N^{12}}{2I_N^{11}}, \quad P_2 = \frac{I_N^{11} + I_N^{12} - 2I_N^{13}}{4I_N^{11}},$$

$$\tau_1 = \frac{1}{2(k_{MR} + k_{SE})}, \quad \tau_2 = \frac{1}{4k_{SE}}.$$

Thus, the exchange decay consists of two components: the characteristic time of one of them is determined by the spin diffusion rate alone, and that of the other by the sum of spin diffusion and molecular reorientation rates. It follows from Eqn (36) that molecular motion can be registered only when it is faster than the spin diffusion rate, i.e., when $k_{MR} \geqslant k_{SE}$. Otherwise, molecular motion is in principle unobservable in an exchange experiment.

As for slow molecular motion in a wet barstar, the analysis of exchange decays at a temperature of $25\,^{\circ}$C and above indicated that the correlation time of the molecular motion at room temperature was dozens and hundreds of milliseconds, and the activation energy varied from 40 to 120 kJ mol$^{-1}$. However, this analysis could give only rough quantitative estimates because separation of the exchange decay into spin diffusion and molecular motion components in this work was made literally 'by eye'.

The nature of exchange decay observed in carbonyl carbons in polyglycine is worth special discussion. Because the shape of the decay showed no temperature dependence, this exchange was also attributed to spin diffusion between $^{13}C$ nuclei. However, we can state now that such an attribution is not quite correct. The natural abundance of $^{13}C$ nuclei is known to be only slightly in excess of one percent, while the mean distance between them in a polypeptide is rather large. The spin diffusion rate showing very strong dependence on the internuclear distance, it could be manifested in the case above only at mixing times on the order of seconds or fractions of a second. As for smaller mixing times, the exchange decay is due here to the dipole interaction of carbons with covalently bonded $^{14}N$ nuclei within a peptide bond. This interaction can modulate the resonance frequency in the same way as CSA tensor reorientation does. The characteristic time of this modulation is determined by the rate of $^{14}N$-nucleus spin hops from one Zeeman level to another, i.e., by the spin–lattice relaxation rate. Because $^{14}N$ nuclei are quadrupole, their relaxation time $T_1$ is rather short, on the order of milliseconds and dozens of milliseconds. This is the so-called RIDER (Relaxation-Induced Dipolar Exchange with Recoupling) effect [35, 36]. Consequently, polypeptide chain dynamics may be studied with the aid of experiments on carbonyl carbons and alpha-carbons only in $^{15}N$-enriched samples (these nuclei have very long $T_1$). Otherwise, the $^{13}C-^{14}N$ interaction must be suppressed in one way or another.

Thus, it was shown in Ref. [30] that solid-state exchange NMR experiments may be an effective tool for the study of protein dynamics in the millisecond range. At the same time, this study demonstrated that spin diffusion can substantially hamper quantitative analysis of the experimental data. Generally speaking, spin diffusion is a very useful property of nuclear magnetism, when NMR spectral lines need to be assigned and protein spatial structure elucidated [37–40]. But it is always an obstacle in molecular dynamics studies. It is responsible for an additional decay component in exchange experiments and averages relaxation times between different nuclei in relaxation experiments, which makes it difficult to obtain selective dynamic information. The simplest method to suppress spin diffusion between such nuclei as $^{15}N$ and $^{13}C$ is proton decoupling — that is, suppression of dipole–dipole interactions of these nuclei with protons. Because spin diffusion between nitrogens (carbons) depends on $^{15}N-^{1}H$ ($^{13}C-^{1}H$) dipole interaction [16], decoupling may substantially slow down its rate. However, it is almost impossible to realize this approach in the majority of solid-state exchange and relaxation experiments because decoupling during seconds or fractions of a second is likely to destroy the amplifier of the spectrometer and cause sample overheating. Moreover, it has been shown that in certain cases decoupling tends to accelerate spin diffusion [41]. Today, the only practical solution to this problem is selective enrichment of proteins in $^{15}N$ and $^{13}C$ isotopes. Besides slowing down spin diffusion, selective labelling also helps to markedly improve the spectral resolution and facilitate the assignment of spectral lines, even though it simultaneously worsens the representativeness of dynamic information.

As mentioned above, all subsequent solid-state exchange NMR studies on biopolymer dynamics were carried out using CODEX pulse sequences [28, 29]. The first experience with the application of these sequences in the investigation of slow protein dynamics was described in Ref. [42]. Experiments were performed with two proteins of a totally different structure, viz. human ubiquitin and hydrogel-ACA. Ubiquitin is a very compact rigid protein with almost 90% of the chain forming the secondary structure, whereas the three-domain ACA protein is composed of a central disordered part and two peripheral rigid domains that can move independently of each other. As in many other works done by the group headed by M Hong (the University of Iowa, USA), the so-called 'selective and extensive' labelling technique was employed to enrich the proteins in $^{13}C$ isotope [43, 44]. In fact, it was semiselective enrichment, in which only ten of the twenty amino acids were labelled. This allowed the researchers to 'rarify' the NMR spectrum and, in conjunction with the wide dispersion of carbon chemical shifts, to propose in specific cases the assignment of spectral peaks to definite types of carbons in certain amino acids. Such an approach does not yield site-specific assignment of spectral lines, i.e., line assignment to definite atoms in the protein globule, but permits in return obtaining more representative information compared to the selective isotope labelling technique. Both ubiquitin and ACA were fully enriched in the isotope $^{15}N$, and semiselectively in the isotope $^{13}C$ (using the above procedure). In this work, the exchange experiment was carried out on $^{15}N$ nuclei but the signal detection was performed on the basis of a carbon signal: prior to FID recording, nitrogen magnetization was transferred to covalently bonded alpha-carbons of the backbone chain. Such a complicated method had to be used for obtaining partial resolution and making possible the assignment of spectral lines, the $^{15}N$ spectrum of a fully enriched sample being of no value for this purpose because the dispersion of isotropic chemical shifts for nitrogens is narrower than for carbons; hence, the spectrum of backbone nitrogens-15 looks like a single broad line. It was eventually discovered that ubiquitin underwent no dynamics in the millisecond range, whereas the ACA protein in the CODEX experiment showed a substantial decay of the mixing time dependence of spectral line intensities with a correlation time of 80 ms. The authors attributed this discrepancy to the different natures of the two proteins.

Here, the question arises: why is there no spin diffusion between the $^{15}N$ nuclei in ubiquitin that was so well apparent in an earlier study on barstar [30]? The most likely explanation for this discrepancy is different MAS rates in the two experiments: 7 and 2 kHz, respectively. The thing is, the MAS rate being much higher than the magnitude of the internuclear dipole interaction expressed in frequency units, MAS leads to the averaging of this interaction. $^{1}H-^{1}H$ and $^{13}C-^{1}H$ interactions are on the order of 20 kHz; therefore, the MAS rate must be at least 40–50 kHz for the averaging to occur. Some authors report to have already achieved such a rate of MAS [45], but these experiments still encounter serious technical difficulties and have not found wide application. The $^{15}N-^{1}H$ interaction amounting approximately to no more than 3 kHz is quite a different case. MAS at 7 kHz is very likely to result in its pronounced averaging. As mentioned above, the spin diffusion rate between nitrogens is to a large extent determined by the dipole interaction of nitrogens with covalently bonded protons. In other words, a high MAS rate may account for the absence of spin diffusion between nitrogen atoms in ubiquitin. It may be conjectured that a high MAS rate can also lead to the suppression of the aforementioned RIDER effect, even though it should be emphasized that no detailed studies into the MAS rate effect

on the strength of $^{15}N-{}^{1}H$ and $^{14}N-{}^{13}C$ interactions has so far been published.

In subsequent works on biopolymer dynamics, solid-state exchange NMR spectroscopy was employed in conjunction with other NMR techniques providing molecular mobility information. The molecular dynamics of the aforementioned ACA protein was the subject of a detailed investigation reported in Ref. [46]. Comparison of carbon spectra obtained by means of cross-polarization from protons and direct excitation of carbons by a simple 90°-pulse demonstrated that the central polyelectrolyte part of the protein had practically isotropic mobility on the microsecond time scale, whereas hard helical side domains remained motionless. Such a comparison of two spectra allows for qualitative evaluation of the $^{1}H-{}^{13}C$ dipole interaction because it is this interaction that underlies the cross-polarization effect. Molecular motion in a sample with a correlation time smaller than the inverse value of the $^{1}H-{}^{13}C$ interaction expressed in frequency units leads to its partial or complete averaging. In this case, cross-polarization is inefficient. At the same time, the efficiency of direct excitation of carbons is independent of their interaction with protons.

The most interesting part of the above work is the analysis of exchange spectroscopy data. As shown in Ref. [42], the CODEX experiment on $^{15}N$ nuclei in this protein records slow motions at room temperature with a correlation time of 80 ms. Because nitrogens were excited by means of cross-relaxation from protons, this slow motion was attributed to the movements of hard end domains of the ACA protein. Both the correlation times and the exchange decay amplitudes were very similar for different spectral lines. It was therefore concluded that this motion reflected domain reorientation as a whole. In order to determine the amplitude and geometric parameters of the motion, the authors quantitatively analyzed the dependence of the exchange decay amplitude (measured at a mixing time much in excess of the correlation time) on the evolution time $t_1$ that, in the CODEX experiment, is defined by the product $mT_R$ (see Fig. 4). Analysis of the dependence of the exchange decay amplitude on the evolution time permits us to obtain much more reliable information about the geometric parameters of the molecular motion, compared with the analysis of decay taking into account only one evolution time. It is an important advantage of the exchange experiment over the NMR relaxation technique and the analysis of the shapes of spectral lines.

The dependences at different amplitudes were theoretically predicted for the following three models: rotation of end domains about their long axis, their isotropic diffusion reorientation, and jumps between two positions. Comparison of experimental and theoretical curves demonstrated that only the first and the third models can adequately explain the experimental findings, whereas the diffusion domain reorientation model does not obviously agree with experimental results. Despite the lack of data for the unambiguous choice of a single molecular motion model most consistent with the real situation, the calculations nonetheless showed that the angular amplitude of motion of hard end domains is approximately 50°, regardless of the type of model.

Studies into the slow molecular dynamics of ACA protein are of interest as providing important information about the properties and structure of hydrogels. The functional role of hard end domains consists in maintaining intermolecular aggregation precluding protein precipitation, whereas the central polyelectrolyte portion of the protein serves as a swelling agent. The slow reorientation of end domains, observed in the work under consideration, in all likelihood reflects hydrogel structure dynamics, i.e., a characteristic time and possible mechanisms of transport of end domains from one aggregate to another. It is natural to hypothesize that the characteristics of this equilibrium dynamic process also dictate many macroscopic physico-chemical properties of hydrogels.

The same group of researchers undertook a detailed study of the molecular dynamics of the membrane protein colicin in the free and membrane-bound states [47]. This protein was also fully labelled with $^{15}N$ isotopes, and semiselectively with $^{13}C$. Alpha-carbons of eight amino acid species and side-chain carbons of two amino acids were identified in the $^{13}C$ spectrum. A battery of NMR techniques was employed in studying molecular motions that provided information about molecular dynamics in different frequency ranges. Constants of $^{13}C-{}^{1}H$ and $^{1}H-{}^{1}H$ dipole–dipole interactions were measured in the DIPSHIFT [48] and WISE [49] experiments, respectively. These constants yielded information about the common amplitude of all motions with correlation times shorter than $10^{-5}$ s. The analysis of the shape of the $^{15}N$ nuclear spectrum in a static sample provided information on the amplitude of backbone chain movements with correlation times shorter than $10^{-4}$ s. In addition, the authors measured proton relaxation times in a coordinate system rotating at the magic angle (the Lee–Goldburg sequence [50]) to obtain information on the molecular dynamics in the microsecond range. In this experiment, the signal was detected on $^{13}C$ nuclei, which ensured selectivity of proton relaxation measurements due to the wide dispersion of carbon chemical shifts. Finally, backbone dynamics in the millisecond range were investigated with the aid of the CODEX experiment on $^{15}N$ nuclei and detection of carbon signals (see the description of this method above) at several mixing times ranging from 1 to 400 ms.

This complex study has demonstrated that colicin undergoes molecular motions with correlation times in the micro- and nanosecond ranges and that protein binding to membranes results in a substantial increase of the amplitudes of both the backbone and side chains. The authors hypothesized that the enhanced mobility of the protein within the membrane constitutes an indispensable condition of its normal functioning, i.e., maintaining the work of membrane channels. It is also worth mentioning that no molecular dynamics in the millisecond range were detected by exchange spectroscopy either in the free or in the membrane-bound state of colicin. Under these experimental conditions, colicin behaved similarly to ubiquitin [42]. This work provides a good example of the application of a wide set of NMR experiments spanning a wide frequency range of molecular motions. However, the results of different experiments in this study, as in the overwhelming majority of other cases, were analyzed independently and compared only at the qualitative level.

In Ref. [51], the molecular dynamics of collagen were studied at different temperatures in the dry and wet states using NMR at a natural abundance of $^{13}C$ nuclei. Motion-averaged constants of $^{13}C-{}^{1}H$ dipole–dipole interaction were measured with the aid of the DIPSHIFT experiment [48], and the CODEX pulse sequence was applied in studying molecular dynamics in the millisecond range. Bearing in mind the RIDER effect, the analysis of spectral line intensities at different mixing times in the CODEX experiment was carried

out only for the spectral lines assigned to beta- and gamma-carbons of prolines and hydroxyprolines because these carbons have no covalently bonded nitrogens. The proportion of prolines and hydroxyprolines in collagen being much higher than in the majority of other proteins, the carbon lines of these residues are resolved in the collagen spectrum. At the same time, the degree of CSA of these carbons is more than four times smaller compared with carboxyl carbons, which accounts for the decreased intensity decay amplitude in the $\tau_m$-dependence. This, in turn, requires a great number of accumulations necessary to ensure a sufficiently large signal-to-noise ratio. For this reason, the study in question compared only two mixing times, 1 ms and 100–200 ms, and thus recorded only the presence of slow molecular motion without providing information about its correlation time. The CODEX experiment demonstrated that slow motions were practically absent in dry collagen, whereas hydroxyprolines in its wet samples exhibited a rather high level of mobility in the millisecond range. $^{13}C-^{1}H$ interaction constants indicated that the amplitude of motion in a higher frequency range was strongly dependent on protein hydration but exhibited only weak dependence on temperature.

An interesting application of the CODEX experiment was described in one of the recent papers published by M Hong group [52]. This work was designed to study molecular dynamics and aggregation of antimicrobial peptide protegrin-1 built into a phospholipid bilayer that served as a model of a biological membrane. Antimicrobial peptides play an important role in the immune system of many living organisms. They destroy cell walls of alien microorganisms. It is supposed that antimicrobial peptides are active only in the aggregated state. One of the parameters used in evaluating the degree and the nature of aggregation of antimicrobial peptides is the correlation time of aggregate rotation in the phospholipid bilayer as a whole.

This correlation time was determined using the CODEX experiment on the carbonyl carbon in one of the amino acids incorporated into protegrin-1 (for the purpose of this experiment, the peptide was selectively enriched in isotope $^{13}C$ at a single chemical site). The correlation time proved to be equal to 0.7 s. The neglect of the RIDER effect in this case was totally justified because the relaxation time $T_1$ of the $^{14}N$ nuclei was at least one order of magnitude shorter.

It turned out to be impossible to describe the slow reorientation of peptide aggregates with the application of the simplest hydrodynamic model based on the Stokes–Einstein equation. In such a case, the size of the aggregates must be improbably large. The authors explained the experimentally found long correlation time of aggregate rotation by the formation of lipid–peptide aggregate complexes and electrostatic interactions between anionic phospholipid heads and cationic side chains of arginines in the protegrin-1 peptide.

In conclusion, it is worth considering one more work in which the intramolecular dynamics of proteins was investigated using solid-state exchange NMR spectroscopy [53]. The main feature of this study was simultaneous quantitative analysis of relaxation and exchange data in the framework of the formalism of correlation functions. This method was termed SREDA (Simultaneous Relaxation and Exchange Data Analysis). It is based on the application of the so-called model-free approach to the analysis of the shape of correlation function of the molecular motion [54, 55]. This approach is currently one of the most widely used methods for the analysis of NMR relaxation data. With this method, the internuclear dipole–dipole interaction (or quadrupolar one if relaxation of quadrupole nuclei is involved) is divided into two parts: one averaged and the other unaveraged by the molecular motion. Complete averaging of the interaction occurs only where isotropic motion is observable in solutions or melts. For obvious reasons, however, intramolecular motions are always more or less anisotropic. The unaveraged portion of the interaction is denoted as a dimensionless order parameter $S^2$ varying from zero (for isotropic motions) to unity (in the absence of motions). The main advantage of the model-free approach consists in permitting the correct description of the shape of the correlation function of the molecular motion without knowing its concrete geometric models (hence, the term 'model-free'). At the same time, a geometric model of motion provides information of paramount importance. First, the knowledge of the model allows the dimensionless order parameter to be recalculated into the amplitude of motion expressed in reorientation angles of the internuclear vector (or the electric field gradient in the case of quadrupole nuclei). Second, the model can by itself provide information about the nature and the mechanisms of the functioning of biomacromolecules. However, it is impossible to choose a model of motion based on standard measurements of NMR relaxation times alone because this procedure is an essentially ambiguous one allowing the same value of the parameter of molecular motion anisotropy to be realized in a variety of geometric models and at different amplitudes.

An almost analogous situation exists in exchange NMR spectroscopy — that is, the experimentally examined dependence of the spectral line amplitude on the mixing time is actually the correlation function of CSA tensor reorientation, from which it is possible to unambiguously determine the correlation time of the molecular motion but not the geometry of CSA tensor reorientation. It is worth noting, however, that the CODEX experiment allows for the selection of different modes by measurements at different periods of evolution $mT_R$, as described in Ref. [46].

Such a selection is possible not only by measurements at different $mT_R$ but also with the aid of simultaneous analysis of exchange and relaxation data. The model-free approach employed in analyzing NMR relaxation times is also applicable to the formal description of the mixing time dependence of the spectral line amplitude, i.e., the correlation function of CSA tensor reorientation. When the internuclear vector and the CSA tensor are rigidly linked to each other, it is natural to expect that the characteristic time of the molecular motions, observed in exchange and relaxation experiments, should be identical. However, the order parameters must by definition be different because they are defined by different formulas

$$S^2_{\text{relax}} = \int_0^{\pi}\int_0^{2\pi}\int_0^{\pi}\int_0^{2\pi} \rho(\theta_1,\varphi_1)\,\rho(\theta_2,\varphi_2) \times \frac{3\left(\mathbf{n}(\theta_1,\varphi_1)\cdot\mathbf{n}(\theta_2,\varphi_2)\right)^2-1}{2}\,\mathrm{d}\varphi_1\,\mathrm{d}\theta_1\,\mathrm{d}\varphi_2\,\mathrm{d}\theta_2\,, \quad (37)$$

$$S^2_{\text{exch}} = \int_0^{\pi}\int_0^{2\pi}\int_0^{\pi}\int_0^{2\pi} \rho(\theta_1,\varphi_1)\,\rho(\theta_2,\varphi_2) \times \frac{I(\theta_1,\varphi_1,\theta_1,\varphi_1)+I(\theta_1,\varphi_1,\theta_2,\varphi_2)}{2I(\theta_1,\varphi_1,\theta_1,\varphi_1)}\,\mathrm{d}\varphi_1\,\mathrm{d}\theta_1\,\mathrm{d}\varphi_2\,\mathrm{d}\theta_2\,, \quad (38)$$

where $\theta$ and $\varphi$ are the standard coordinates of the polar frame of reference; $\rho(\theta, \varphi)$ is the distribution function of internuclear vector orientations (of the CSA tensor principal axis) that determines the geometric model of motion; $\mathbf{n}(\theta, \varphi)$ is the unit vector, the direction of which is given by the angles $\theta$ and $\varphi$, and $I(\theta_a, \varphi_a, \theta_b, \varphi_b)$ is the amplitude of a spectral line in the exchange NMR spectrum under the condition that orientation of the principal axis of the CSA tensor before and after the mixing time is given by angular coordinates $(\theta_a, \varphi_a)$ and $(\theta_b, \varphi_b)$, respectively.

The quantity $I(\theta_a, \varphi_a, \theta_b, \varphi_b)$ is found from the mathematical formalism described above. Motion models [i.e., orientational distribution functions $\rho(\theta, \varphi)$] are selected bearing in mind that they must satisfy the results of two experiments taken together, substantially reducing the uncertainty in its choice but not completely excluding it. It should be emphasized that such an algorithm is completely correct only on the assumption of axial symmetry of the CSA tensor and of coincident directions of the internuclear vector and the principal axis of the CSA tensor. Nitrogen nuclei in the protein backbone appear to most strictly satisfy this condition. Their CSA tensor is almost axially symmetric and the difference between the directions of the N–H vector and the principal axis of the CSA tensor does not exceed 20° [56]; therefore, it can be neglected in the first approximation.

Such an analytical algorithm was applied in Ref. [53], which describes the molecular dynamics of the barstar backbone in the free and binase-bound states investigated with the aid of NMR spectroscopy on $^{15}$N nuclei. In order to slow down the spin diffusion rate observed in the fully $^{15}$N-enriched protein in a previous experiment [30], only 15% enrichment of barstar was undertaken, which resulted in the dilution of the spin system and an increase in the mean distance between the $^{15}$N nuclei. If the results of the exchange and relaxation experiments are to be compared, they must be sensitive to a roughly identical frequency range of molecular dynamics. Evidently, the measurement of the NMR relaxation time $T_1$ is not suitable for this purpose because this time depends on the molecular dynamics in the nanosecond range, whereas exchange spectroscopy provides information about millisecond motions (although relaxation times $T_1$ were also measured in this work for the investigation of high-frequency dynamics). Such a study requires the measurement of relaxation time $T_{1\rho}$ in the rotating frame of reference that is normally susceptible to motions with correlation times on the order of dozens and hundreds of microseconds. In the work under consideration, the relaxation time $T_{1\rho}$ was measured in the tilted coordinate system — that is, by means of resonance offset of the spin-lock field [57]. This measuring technique allows the spin-lock field to be enlarged without increasing the transmitter power, and as a consequence to exclude an additional spin–spin contribution to the relaxation rate, which frequently makes the measurements of the relaxation time $T_{1\rho}$ of little value for the investigation into molecular dynamics [58].

In order to analyze the data obtained in this work, the authors calculated the order parameters $S^2_{\text{relax}}$ and $S^2_{\text{exch}}$ [see Eqns (37) and (38)] for several models of motion at different angular amplitudes. It turned out that this dependence is different for different models if one order parameter is expressed via the other, as shown in Fig. 6. It should be borne in mind that if $S^2_{\text{relax}}$ is determined by the motion itself, then $S^2_{\text{exch}}$ also depends on CSA tensor parameters, the resonance frequency, and the evolution period of the exchange experiment. Therefore, a change in any of these parameters would result in the altered shape of the curves in Fig. 6. The figure shows that the difference between the models is especially well-apparent at high motion amplitudes (low order parameters); when the amplitudes are small, it is impossible to distinguish one model from another because of experimental errors.

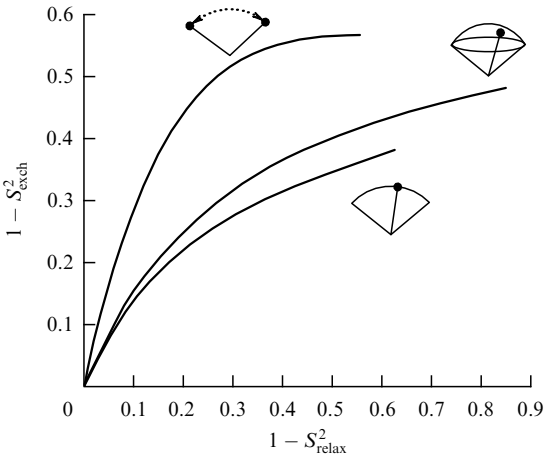


**Figure 6.** Calculated interdependence of the order parameters corresponding to exchange (CODEX pulse sequence) and relaxation experiments at different angular amplitudes of the motion for three models: jumps between two equally probable orientations (top), diffusion reorientation within a cone (middle), and diffusion reorientation within a planar angle (bottom). The calculations were done for $^{15}$N nuclei at the following values of the experimental parameters: resonance frequency for nitrogens — 40.5 MHz, MAS frequency — 3 kHz, evolution period — 0.33 ms ($m = 1$, see Fig. 4), and CSA ($\sigma_{11} - \sigma_{33}$) — 160 ppm.

Simultaneous analysis of relaxation and exchange data demonstrated that the backbone chain of barstar participates in two types of molecular motions with correlation times on the order of $10^{-9}-10^{-7}$ s and $10^{-3}-10^{-2}$ s. Formation of the barstar–binase complex results in a decrease in the amplitudes of both motions. The analysis of different models of motion revealed that experimental data were best described by the wobbling-in-a-cone model, even though the experimental errors precluded an unambiguous choice in favor of one model or another. Because it is impossible to obtain high resolution in a one-dimensional solid-state NMR spectrum in the case of nonspecific isotope enrichment of the sample, the data obtained refer to molecular dynamics averaged over all amino acid residues. From this standpoint, selective enrichment of proteins and site-specific assignment of spectral lines would substantially increase the value of molecular dynamic information. However, such experiments are very laborious because a weak NMR signal dictates the necessity of time-consuming measurements.

## 4. Conclusions

By virtue of certain methodical modifications, one-dimensional solid-state exchange NMR spectroscopy with MAS has become a powerful and informative experimental tool for the investigation into the dynamics of various molecular systems. The information available with the aid of this NMR experiment is in many respects unique.

The uniqueness is, first and foremost, due to a wide range of correlation times of molecular motions, varying from

fractions of a millisecond to units or dozens of seconds. Molecular motions in this range have until recently been surveyed largely by indirect methods, such as the hydrogen exchange technique. The broad range of correlation times is of special value for the study of biomacromolecules because it is characteristic of many biological processes.

Second, there is a unique possibility to obtain the correlation function of reorientational motion directly from experiment, without resorting to numerical simulation. In the case of NMR relaxation or analysis of NMR spectral line shape, the determination of the shape of the correlation function almost invariably requires the employment of some approximations or assumptions. Finally, exchange spectroscopy permits us to study not only the mixing time dependence but also the dependence on the evolution time and thus to obtain more definitive information about geometric models of molecular motions than by means of NMR relaxation and line shape analysis. The possibility of analyzing the geometry of the molecular motion may be substantially enhanced by combined quantitative analysis of data on exchange and relaxation NMR spectroscopies [53].

The main methodical drawback of exchange NMR spectroscopy lies in the fact that it is less suitable for the study of low-amplitude molecular motions compared with relaxation experiments. In the case of relaxation, a decrease in the motion amplitude leads to the prolongation of the relaxation time. Nevertheless, it can be measured as accurately as a shorter relaxation time, whereas the detection of low-amplitude motions in exchange experiments requires practically precise measurements of NMR spectral line amplitudes, which is sometimes difficult to make under real experimental conditions.

The first and still rare examples of the application of the solid-state exchange spectroscopy to the investigation of low-frequency conformational dynamics of proteins have demonstrated that these dynamics are manifested differently in various proteins and under different experimental conditions. Evidently, the amplitude of these dynamics may depend on hydration [30, 51] of the protein and its binding to a substrate [53]. It should be emphasized that in such proteins as colicin and ubiquitin the internal dynamics in the millisecond range were virtually absent [42, 47]. On the one hand, they may be accounted for by specific features of these proteins and, on the other hand, by the methodical problem mentioned in the preceding paragraph. This question has not yet been cleared up. It is worth noting that the CODEX pulse sequence has been successfully used during the last few years in studies of the dynamics of synthetic polymers where molecular motions in the millisecond range were recorded without any serious difficulty [59 – 62]. However, synthetic polymers are normally lacking a rigid spatial structure inherent in globular proteins; therefore, amplitudes of their slow motions can be much larger, which makes it easier to observe them in the exchange experiment.

In conclusion, a few notes are in order on those lines of experimental NMR studies of protein dynamics, in which solid-state exchange spectroscopy has not so far been used but may prove to be very useful in further surveys.

First, no experiment has thus far been reported on a selectively isotope-labelled protein with a site-specific resolution of its NMR spectrum. The exception is Ref. [52] but selective enrichment in this study did not make much sense for exchange spectroscopy because it was applied to the detection of the rotation of peptide aggregates as a whole. Selectively labelled proteins have long been used in both relaxation NMR experiments [63, 64] and experiments undertaken for line shape analysis [63 – 66], even though the number of such studies is still very small. There is little doubt that highly localized dynamic information is of much greater interest for understanding the properties and the nature of the biological functioning of proteins than information averaged over a group of atoms.

Second, no experiment has yet been carried out in which simultaneous quantitative analysis of exchange data and the NMR spectrum shape was performed either for a static sample or for a sample rotating at the magic angle. As in the SREDA method [53], such an analysis would doubtlessly provide more reliable information about the nature and geometry of slow molecular motions. Equally promising is a modification of the SREDA method, in which NMR relaxation times are analyzed concurrently with the dependences on mixing time and evolution period. Finally, the most detailed information on the nature of molecular motions might be obtained by means of a combined analysis of all the three NMR methods — that is, exchange, line shape analysis, and relaxation. No such works have yet been reported.

Third, no solid-state exchange NMR experiment has so far been carried out in proteins on deuterium nuclei. Experiments with the use of deuterium may be of interest because deuterium possesses the most anisotropic CSA tensor; hence, these nuclei must be highly sensitive to low-amplitude motions. Deuterium exhibits a relatively short spin – lattice relaxation time (usually hundreds of milliseconds), which somewhat narrows the frequency range of the studies; nevertheless, deuterium nuclei are most optimal for simultaneous experimental studies of molecular dynamics by all three NMR methods mentioned above.

The main obstacle that hampers all these experiments is their being costly and lengthy. Such complex experiments may last months (taking into account only the time of NMR spectrometer operation, without regard for the time necessary to treat the data obtained). Modern high-field spectrometers with a resonance frequency for protons above 500 – 600 MHz are needed to carry out such studies. Hence, only a few laboratories can afford them at present. For all that, we believe that only such a complex approach can ensure a breakthrough in this field of molecular biophysics in the near future.

The author is grateful to Dr. Detlef Reichert, his friend and colleague, with whom joint work over many years made possible the appearance of this review.

## References

1. Perutz M et al. *Nature* **185** 416 (1960)
2. Wüthrich K *NMR of Proteins and Nucleic Acids* (New York: Wiley, 1986)
3. Karplus M *J. Phys. Chem. B* **104** 11 (2000)
4. Buckle A M, Schreiber G, Fersht A R *Biochemistry* **33** 8878 (1994)
5. Wong K-B, Fersht A R, Freund S M V *J. Mol. Biol.* **268** 494 (1997)
6. Gryk M R, Jardetzky O *J. Mol. Biol.* **255** 204 (1996)
7. Gabel F et al. *Quart. Rev. Biophys.* **35** 327 (2002)
8. Parak F G *Rep. Prog. Phys.* **66** 103 (2003)
9. Sinha N, Smith-Gill S J *Prot. Pept. Lett.* **9** 367 (2002)
10. Wand A J *Nature Struct. Biol.* **8** 926 (2001)
11. Kempf J G, Loria J P *Cell Biochem. Biophys.* **37** 187 (2003)
12. Palmer A G (III), Williams J, McDermott A *J. Phys. Chem.* **100** 13293 (1996)

13. Palmer A G (III), Kroenke C D, Loria J P *Methods Enzymol.* **339** 204 (2001)
14. Abragam A *The Principles of Nuclear Magnetism* (Oxford: Clarendon Press, 1961)
15. Slichter C P *Principles of Magnetic Resonance* 2nd ed. (Berlin: Springer-Verlag, 1978)
16. Schmidt-Rohr K, Spiess H *Multidimensional Solid-State NMR and Polymers* (London: Academic Press, 1994)
17. Jeener J et al. *J. Chem. Phys.* **71** 4546 (1979)
18. Hagemeyer A et al. *Chem. Phys. Lett.* **167** 583 (1990)
19. Andrew E R, Bradbury A, Eades R G *Nature* **182** 1659 (1958)
20. Szeverenyi N M, Sullivan M J, Maciel G E *J. Magn. Reson.* **47** 462 (1982)
21. Pines A, Gibby M G, Waugh J S *J. Chem. Phys.* **56** 1776 (1972)
22. Luz Z, Tekely P, Reichert D *Prog. Nucl. Magn. Reson. Spectrosc.* **41** 83 (2002)
23. Gérardy-Montouillout V et al. *J. Magn. Reson. A* **123** 7 (1996)
24. Reichert D et al. *J. Magn. Reson.* **125** 245 (1997)
25. Tekely P et al. *J. Magn. Reson.* **145** 173 (2000)
26. Favre D E, Schaefer D J, Chmelka B F *J. Magn. Reson.* **134** 261 (1998)
27. Reichert D et al. *J. Magn. Reson.* **146** 311 (2000)
28. deAzevedo E et al. *J. Am. Chem. Soc.* **121** 8411 (1999)
29. deAzevedo E R et al. *J. Chem. Phys.* **112** 8988 (2000)
30. Krushelnitsky A et al. *J. Magn. Reson.* **138** 244 (1999)
31. Siminovitch D J *Biochem. Cell Biol.* **76** 411 (1998)
32. Rupley J, Careri G *Adv. Prot. Chem.* **41** 37 (1991)
33. Belton P S *Prog. Biophys. Mol. Biol.* **61** 61 (1994)
34. Torchia D A *J. Magn. Reson.* **30** 613 (1978)
35. Weliky D P, Tycko R *J. Am. Chem. Soc.* **118** 8487 (1996)
36. Saalwächter K, Schmidt-Rohr K *J. Magn. Reson.* **145** 161 (2000)
37. McDermott A et al. *J. Biomol. NMR* **16** 209 (2000)
38. McDermott A, in *Protein NMR for the Millennium* (Biological Magnetic Resonance, Vol. 20, Eds N R Krishna, L J Berliner) (New York: Kluwer Acad./Plenum Publ., 2003) p. 103
39. Pauli J et al. *ChemBioChem* **2** 272 (2001)
40. Castellani F et al. *Nature* **420** 98 (2002)
41. Reichert D et al. *Solid State Nucl. Magn. Reson.* **13** 137 (1998)
42. deAzevedo E R, Kennedy S B, Hong M *Chem. Phys. Lett.* **321** 43 (2000)
43. Hong M, Jakes K *J. Biomol. NMR* **14** 71 (1999)
44. Hong M *J. Magn. Reson.* **139** 389 (1999)
45. Ernst M et al. *J. Am. Chem. Soc.* **126** 4764 (2004)
46. Kennedy S B et al. *Macromolecules* **34** 8675 (2001)
47. Huster D, Xiao L, Hong M *Biochemistry* **40** 7662 (2001)
48. Kolbert A C et al., in *Multinuclear Magnetic Resonance in Liquids and Solids*: *Chemical Applications* (NATO ASI Ser., Ser. C, No. 322, Eds P Granger, R K Harris) (Dordrecht: Kluwer Acad. Publ., 1990) p. 339
49. Schmidt-Rohr K, Clauss J, Spiess H W *Macromolecules* **25** 3273 (1992)
50. van Rossum B-J et al. *J. Am. Chem. Soc.* **122** 3465 (2000)
51. Reichert D et al. *Magn. Reson. Chem.* **42** 276 (2004)
52. Buffy J J et al. *Biochemistry* **42** 13725 (2003)
53. Krushelnitsky A G, Hempel G, Reichert D *Biochim. Biophys. Acta*: *Prot. Proteom.* **1650** 117 (2003)
54. Lipari G, Szabo A *J. Am. Chem. Soc.* **104** 4546 (1982)
55. Lipari G, Szabo A *J. Am. Chem. Soc.* **104** 4559 (1982)
56. Oas T G et al. *J. Am. Chem. Soc.* **109** 5956 (1987)
57. Krushelnitsky A et al. *Solid State Nucl. Magn. Reson.* **22** 423 (2002)
58. Van der Hart D L, Garroway A N *J. Chem. Phys.* **71** 2773 (1979)
59. Bonagamba T J et al. *J. Polymer Sci. B*: *Polymer Phys.* **39** 2444 (2001)
60. Miyoshi T, Pascui O, Reichert D *Macromolecules* **35** 7178 (2002)
61. Pascui O, Beiner M, Reichert D *Macromolecules* **36** 3992 (2003)
62. deAzevedo E R et al. *J. Chem. Phys.* **119** 2923 (2003)
63. Tamura A et al. *Protein Sci.* **5** 127 (1996)
64. Cole H B R, Torchia D A *Chem. Phys.* **158** 271 (1991)
65. Williams J C, McDermott A E *Biochemistry* **34** 8309 (1995)
66. Shaw W J et al. *J. Am. Chem. Soc.* **122** 7118 (2000)